

## **The CrO<sub>x</sub> / SiO<sub>2</sub> / Si(100) Catalyst - A Surface Science Approach to Supported Olefin Polymerization Catalysis**

P.C. Thüne<sup>1,2</sup>, J. Loos<sup>2</sup>, D. Wouters<sup>1</sup>, P.J. Lemstra<sup>2</sup> and J.W. Niemantsverdriet<sup>\*</sup>

1) Schuit Institute of Catalysis

2) Dutch Polymer Institute

Eindhoven University of Technology, Eindhoven, The Netherlands

**SUMMARY:** Depositing catalytically active particles onto flat, thin and oxidic support forms an attractive way to make supported catalyst suitable for surface science characterization. Here we show how this approach has been applied to the Phillips (CrO<sub>x</sub> / SiO<sub>2</sub>) ethylene polymerization catalyst. The model catalyst shows a respectable polymerization activity after thermal activation in dry air (calcination). Combining the molecular information from X-ray Photoelectron Spectroscopy (XPS) and Secondary Ion Mass Spectrometry (SIMS) we can draw a molecular level of the activated catalyst that features exclusively monochromate species, which are anchored to the silica support via ester bonds with the surface silanol groups. These surface chromates form the active polymerization site upon contact with ethylene. Upon increasing calcination temperature we observe a decrease in chromium coverage as some of the surface chromate desorbs from the silica surface. Nevertheless, we also find an increasing polymerization activity of the model catalyst. We attribute this increase in catalytic activity to the isolation of the supported chromium, which prevents dimerization of the coordinatively unsaturated active site. Diluting the amount of chromium to 200 Cr-atoms/nm<sup>2</sup> of silica surface enables the visualisation of polyethylene produced by a single active site.

### **1. Introduction**

#### **The heterogeneous model catalyst approach**

Generally speaking a model catalyst is an idealized version of a real (heterogeneous) catalytic system that has been prepared to gain information, which cannot be obtained using the real system. A model is much simpler than the industrial catalyst: the industrial support is removed or altered, promoting agents and structural aids are missing. This is done to meet demands of spectroscopic and microscopic techniques and to limit the amount of unknown parameters in the system. Model catalysts are prepared as a compromise between two contradictory demands: The desire to achieve atomic definition and control of the surface and the need to resemble the industrial original to maintain relevance and credibility. Model catalysts can be homogeneous, based on well defined organometallic compounds or only exist

as a computer algorithm, but for this introduction we will restrict ourselves to heterogeneous model catalysts<sup>1,2)</sup> that are optimized for the application of surface science and microscopic probes<sup>3,4)</sup>.

Ultimate definition models for the active phase are single crystals, with a known geometry of surface atoms depending on direction of the cleavage and the crystal. A whole battery of powerful surface analysis techniques has developed in the past decades, most of them demand ultra high vacuum (UHV) but a few are also applicable at higher pressures and in some cases under reaction conditions<sup>3,4)</sup>. However, more often than not single crystals provide only little resemblance to a true catalyst, they are sometimes not even active. This is because the active phase on a “real” catalyst is finely dispersed on the support. Metallic (or non-metallic) clusters of a few nanometers are common and sometimes we find even isolated molecules as active sites, for example, on the Phillips catalyst ( $\text{CrO}_x / \text{SiO}_2$ ). An attempt to incorporate more real world catalysis is made using “model supports” like alumina or silica usually, which are applied as thin films on conducting structural supports. Again two approaches exist emphasizing control or similarity to the industrial catalyst. If hardcore surface science background dictates definition, typical surface science preparation techniques are employed like (reactive) evaporation<sup>5)</sup> or electron beam lithography<sup>6-8)</sup>. Magni and Somorjai used this approach to model Ziegler-Natta polymerization catalysts<sup>9)</sup>

If more emphasis is laid on resemblance to “real life” heterogeneous catalysts, one strives to imitate the industrial catalyst preparation as closely as possible in order to maintain the same surface chemistry as on the industrial complement. The model support, often a flat silicon wafer (a  $\text{Si}(100)$  single crystal covered with a flat, thin film of  $\text{SiO}_2$ ), is loaded with the active phase with a wet impregnation technique called spincoating<sup>10-12)</sup> that imitates the widely applied pore volume impregnation used on porous supports like silica gel.

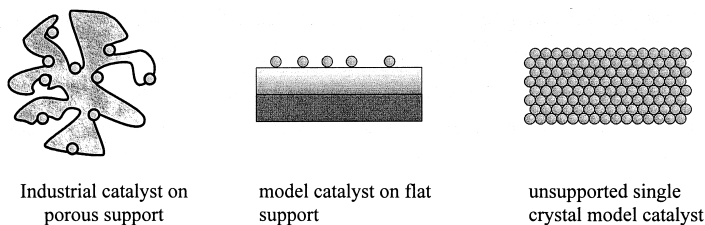


Fig. 1: Schematic drawings of (left) a conventional, porous catalyst; (middle) a model supported catalyst with catalytically active phase on a thin layer of support-like material and a flat conducting substrate; (right) a well defined single crystal model of the supported phase, redrawn from ref<sup>1)</sup>.

The further pretreatment follows the industrial recipe as closely possible (e.g. by thermal treatment in air often called calcination) and finally the catalyst is tested for catalytic activity in much the same way as the industrial counterpart. The molecular state of the active surface is monitored at molecular level detail using surface science techniques such as X-ray Photoelectron Spectroscopy (XPS), Secondary Ion Mass Spectroscopy (SIMS) and Atomic Force Microscopy (AFM)<sup>3)</sup>. The ultimate goal of this approach is to link the preparation parameters to a molecular structure of the catalyst and to the catalytic performance<sup>14)</sup>. This approach has already successfully been applied to model hydrodesulfurization catalysts of the CoMoS type<sup>15)</sup>.

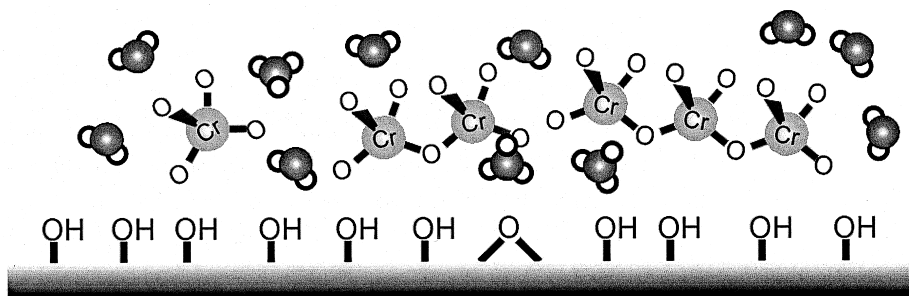
The ultimate goal of this surface science characterization is to create a molecular level picture of the active surface. However, whereas surface spectroscopy and microscopy benefit from the flat, conducting model support, the small catalytically active surface makes it extremely vulnerable for impurities when running catalytic reaction under atmospheric pressure, making the measurement of reproducible catalytic activities the greatest challenge for investigating model catalysts. Nevertheless catalytic testing is essential: only if the model catalyst displays a catalytic activity that resembles that of the industrial counterpart it may claim relevance for the industrial system.

### **The Phillips Catalyst and our model**

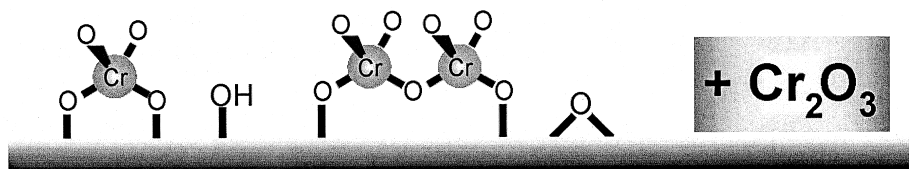
The Phillips catalyst has been discovered by Hogan and Banks<sup>16)</sup> at the Phillips Petroleum Company in the early '50s. Today about one third of all high density polyethylene (HDPE) and Linear Low Density polyethylene (LLDPE) is made using Phillips catalysts. The original recipe involved aqueous impregnation of chromic acid on silica, but nowadays less poisonous chromium(III) salts are used. The impregnated catalyst is further calcined in dry air, to form the active catalyst. Over the years a family of Phillips type catalysts has emerged producing no less than 50 different polyethylenes. This versatility is one of the reasons for the commercial success of the Phillips ethylene polymerization process. The properties of the desired product can be tailored varying parameters like calcination temperature, polymerization temperature and pressure or by variations in the oxidic support e.g. adding titania or simply varying the pore size. However, the sensitivity of the catalyst's performance to details in its preparation has also contributed a great deal to the uncertainty surrounding the characteristics of the supported chromium, the structure of the active site and the mechanism of ethylene polymerization<sup>17,18)</sup>.

The reason for this lies probably in the complex redox and coordination chemistry of chromium in combination with the heterogeneous silica surface. As a result the supported chromium may be present on the support in a mixture of different valences and coordination environments, depending on the exact preparation. This makes comparison between different

a) after impregnation

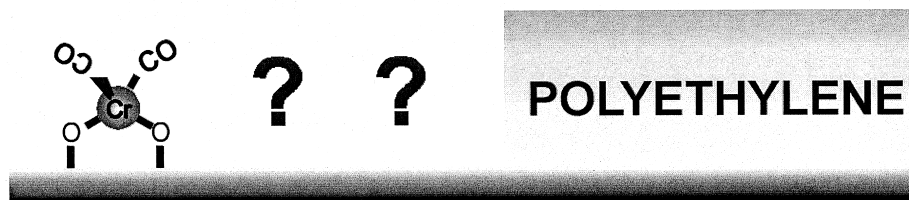


b) after thermal activation



c) reduction with CO

d) with ethylene

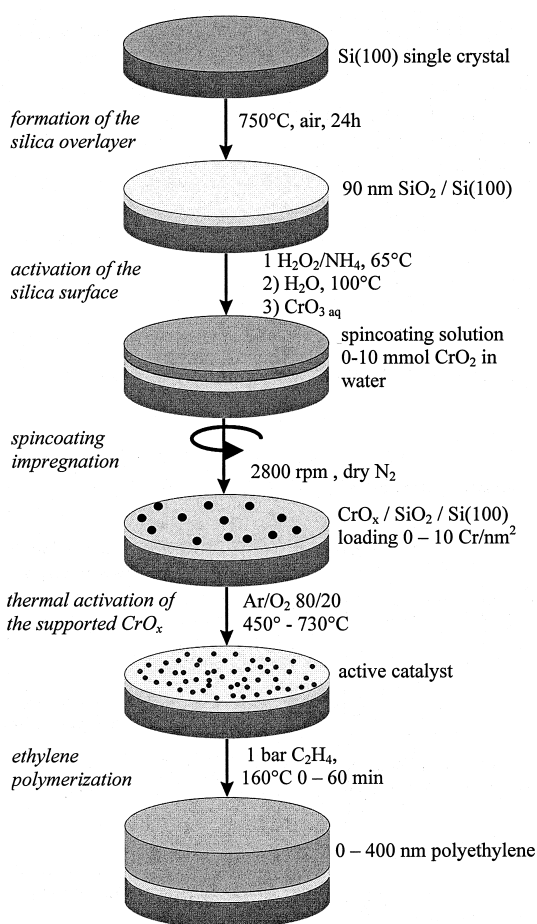


Scheme 1:

After impregnation with aqueous chromic acid (a) an equilibrium mixture of mono-, di-, and polychromates lay on the fully hydroxylized silica support embedded in a water matrix. Upon calcination water desorbs and the chromium forms surface chromates in an esterification reaction with the surface silanol groups (b). Whether these surface chromates also form dimers, etc. is not yet clear. We show later in this article that the monochromate is the precursor for the active polymerization site. Calcination above 500°C yields an active ethylene polymerization catalyst. The surface chromate can be quantitatively reduced to chromium(II) with CO at 350°C (c)<sup>13</sup>. Upon contact with ethylene (d) at temperatures above 60°C the anchored chromate is reduced, probably to a Cr(II) species.

groups very difficult and has prevented the development of a unifying picture of the Phillips Catalyst. The molecular structure of the anchored chromium is still controversial: monochromates, dichromates and even polychromates have been proposed<sup>16,17</sup>.

Polymerization (slurry or gas-phase, 15-20 bar ethylene pressure, around 100°C) of ethylene alone gives a linear polymer without long chain branching (HDPE) while copolymerization of C<sub>4</sub>-C<sub>8</sub> olefins gives a branched polymer (LLDPE). The Phillips catalyst features as little as 1 wt% of chromium on a large pore silica gel, which corresponds to an average coverage of less than 1 Cr/nm<sup>2</sup>. To visualize such a small amount of chromium presents somewhat of a challenge to the surface spectroscopist. For this purpose a flat catalyst with all active phase accessible to surface characterization represents a significant advantage. **Scheme 1** briefly summarizes the surface chemistry of the Phillips Catalyst, **Scheme 2** illustrates the



Scheme 2:

Preparation, activation and testing of the CrO<sub>x</sub> / SiO<sub>2</sub> / Si(100) model catalyst.

preparation and testing of our  $\text{CrO}_x / \text{SiO}_2 / \text{Si}(100)$  model catalyst. In the following we want to show some highlights of our work illustrating how the flat model catalyst approach enables one to look at olefin polymerization catalysis from a somewhat different angle. We will concentrate on the thermal activation of the supported chromium and how it affects the catalytic activity.

## 2. Thermal activation of the $\text{CrO}_x / \text{SiO}_2 / \text{Si}(100)$ model catalyst

Upon calcination the supported chromium anchors to the silica support in an esterification reaction with the surface hydroxyl- groups yielding surface chromate(VI). The maximum amount of chromate that is anchored to the support is limited by the amount of hydroxyls available and decreases with increasing temperature (if lower valent chromium precursors have been impregnated the chromium will be oxidized during the calcination). If a fully hydroxylized silica is used the saturation coverage of anchored chromium(VI) at  $425^\circ\text{C}$  is about  $1.8 - 2.3 \text{ Cr/nm}^2$ , the excess chrome is converted to chromium(III)-oxide<sup>17)</sup>.

While there is general consensus that the surface chromate is the direct precursor of the active polymerization site of the Phillips catalyst, its structure remained disputed in the literature over the years. Indirect evidence has been deduced from measuring the change in hydroxyl population upon binding of the chromium or by the reverse reaction, stripping of anchored chromium using hydrogen chloride<sup>17-20)</sup>. The general trend in these experiments is that chromate anchors to the silica surface initially as monochromate while high calcination temperatures and loadings encourage the formation of dichromates as well as the formation of chromium oxide clusters. These clusters evolve when there are not enough surface silanol groups present on the surface to bind all chromium. Spectroscopic characterization using Raman -, or UV-Vis spectroscopy<sup>21,22)</sup> (and references therein) gave similar results.

We have investigated the effect of calcination on the molecular structure of the supported chromium on our model catalyst using X-ray Photoelectron Spectroscopy (XPS), Secondary Ion Mass Spectrometry (SIMS) and Rutherford Backscattering Spectrometry (RBS)<sup>23-25)</sup>. In many ways the  $\text{CrO}_x / \text{SiO}_2 / \text{Si}(100)$  catalyst behaves as its industrial counterpart. With XPS we can follow the formation of surface esters that consume surface hydroxyl groups of the silica support (**Figure 1**). The amount of chromate, which can be anchored to the silica support in such a fashion, depends on the amount of available surface hydroxyls and decreases with calcination temperature. However, unlike on porous high surface area silicas, we do not observe the transformation of excess chromate to  $\text{Cr}_2\text{O}_3$  at temperatures above  $450^\circ\text{C}$  on our model catalyst. Instead superficial chromium desorbs from the silica surface (**Figure 2**). As a consequence calcination above  $450^\circ\text{C}$  produces catalysts exposing a silica surface, on which all chromium observed using XPS and SIMS is anchored to surface silanols. The rest has desorbed. In addition we find strong evidence that chromate can only bind to the silica surface as a monomeric unit, as all  $\text{Cr}_2\text{O}_3$ -free catalyst show the same  $\text{Cr}2p_{3/2}$  binding energy at  $581.4 \text{ eV}$  independent of chromium loading or calcination

temperature. This suggests that only one chromate species is stable on the silica surface. While SIMS easily detects dimeric  $\text{Cr}_2\text{O}_x^-$  clusterions on reference catalysts containing  $\text{Cr}_2\text{O}_3$ -clusters, we find exclusively monomeric  $\text{CrO}_x$ -clusters on the calcined model catalysts even at chromium loadings above the nominal saturation coverage (**Figure 3**).

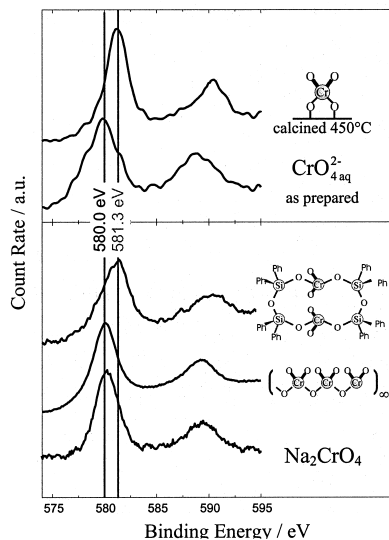


Fig. 1: Cr 2p spectra of the  $\text{CrO}_x/\text{SiO}_2/\text{Si}(100)$  model catalyst and of some chromate(VI) - type reference compounds. Impregnated chromate features the same binding energy as alkali chromates/dichromates or bulk  $\text{CrO}_3$ . Upon calcination this binding energy increases by 1.3 eV. This unusually high binding energy is typical for chromate(VI) forming ester bonds to silica as in  $[\text{CrO}_2(\text{OSi}(\text{C}_6\text{H}_5)_2\text{OSi}(\text{C}_6\text{H}_5)_2\text{O})]_2$  and has no parallel for chromate on other oxidic supports.

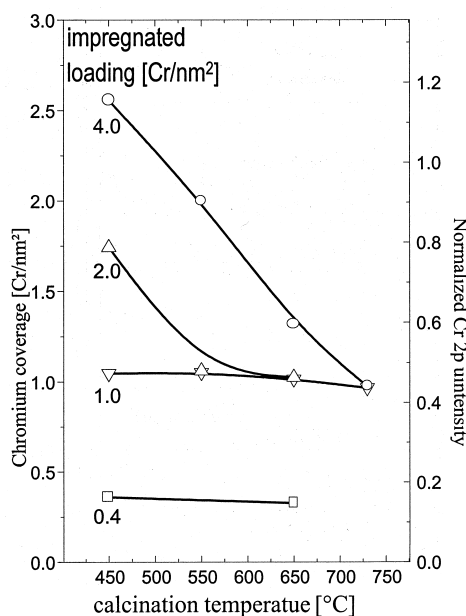


Fig. 2: The chromium coverage decreases with increasing calcination temperature, however at low initial loadings the Cr coverage is much more stable with respect to high calcination temperatures. We assign the decrease in Cr coverage to desorption of chromate, which happens most easily from highly occupied surfaces. Peak shape and position of the Cr2p emission remain constant, implying that chromium forms only one type of surface chromate independent of chromium loading and calcination temperature.

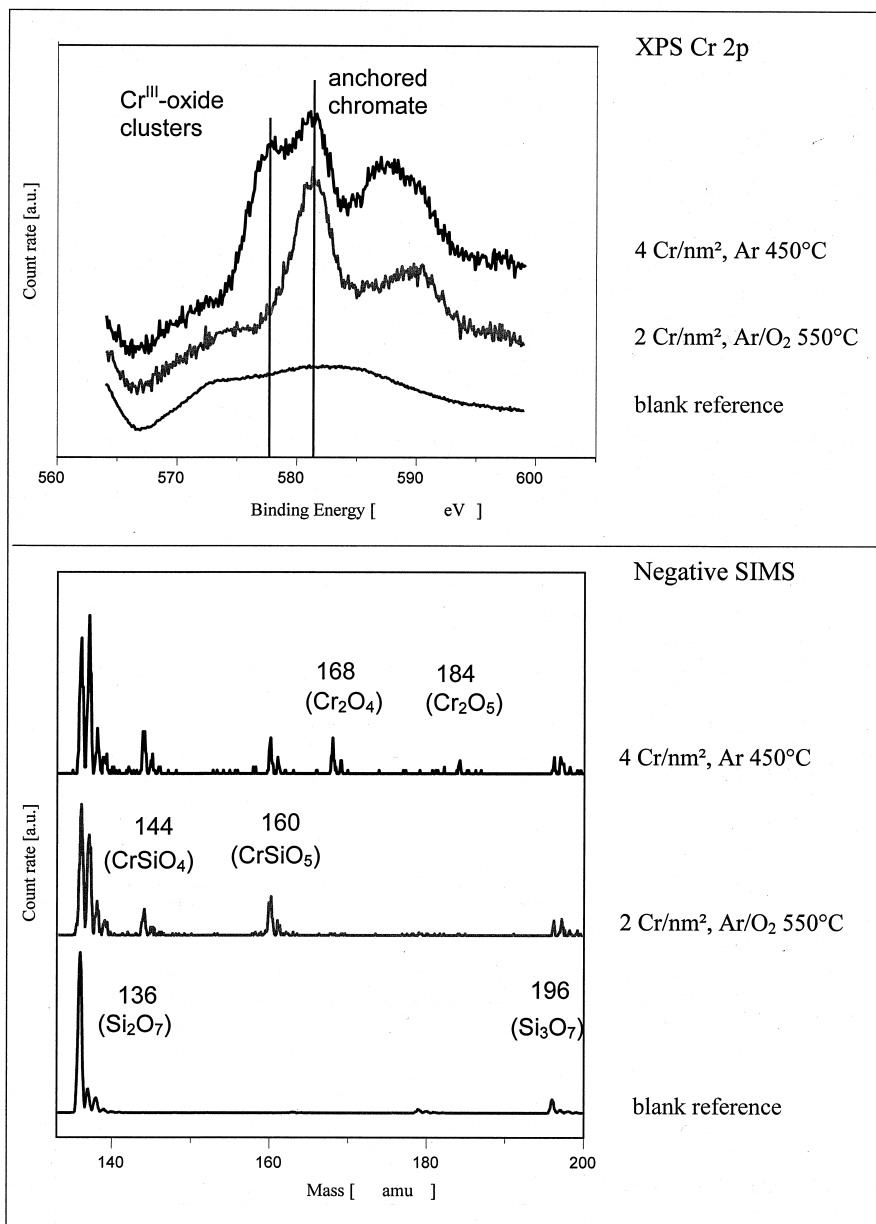


Fig. 3: Cr 2p spectra and negative SIMS spectra of two model catalysts and a blank reference. The blank (bottom) shows only  $\text{Si}_x\text{O}_y$  fragments, on a chromium loaded catalyst  $\text{Cr}_1\text{O}_x$  fragments appear after thermal activation ( $\text{Ar}/\text{O}_2$ ). If desorption of chromium is made impossible (in oxygen free argon) also  $\text{Cr}_2\text{O}_x$  clusters can be detected. In combination this forms strong evidence that chromate anchors to the silica surface as a monomer.



### 3. What kind of polymer does the $\text{CrO}_x / \text{SiO}_2 / \text{Si}(100)$ model catalyst produce?

If a calcined model catalyst is treated with atmospheric ethylene at  $160^\circ\text{C}$ , it immediately develops polymer, which forms a thin, molten film visible to the eye by Newton colors. Obviously this polymer is polyethylene, however, the exact type of polyethylene is uncertain. The catalytic performance of the Phillips catalyst and the properties of the polymer product are very sensitive towards the exact recipe of the catalyst and the mode of polymerization. Even if pure ethylene is used as feedstock the produced polyethylene may vary in molecular weight and in molecular weight distribution. Side reactions during chain growths may induce methyl- or even long chain branching<sup>17</sup>.

These branching reactions are very slow compared to the normal insertion of ethylene. However, even minute amounts of these side branches can have an enormous influence on the polymer properties e.g. on its crystallinity. The probability for chain branching is again dependent on the polymerization parameters. While insertion of a monomer is first order in monomer concentration, the termination reaction ( $\beta$ -H elimination) and chain branching are independent of the ethylene concentration. Especially methyl branching becomes more common if the polymerization is carried out at atmospheric pressure or less. Evidently it is very desirable to study the primary structure of the polymer particles as it determines the quality of the produced polymer and it reflects an essential part of the catalyst reactivity.

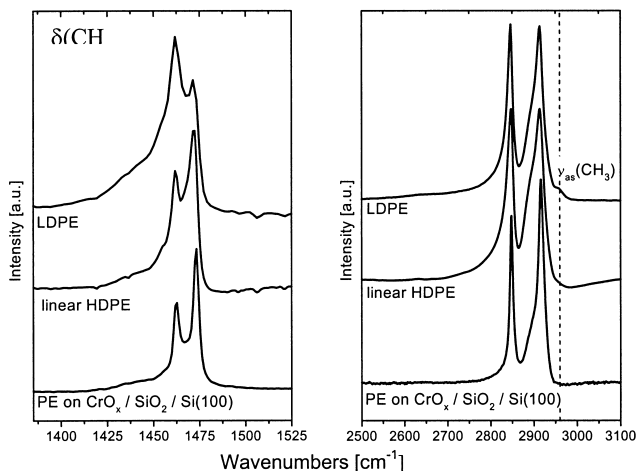


Fig. 4: ATR-IR spectra of branched LDPE (top), linear HDPE (middle) and PE as produced on the  $\text{CrO}_x / \text{SiO}_2 / \text{Si}(100)$  model catalyst ( $160^\circ\text{C}$ , 1 atm  $\text{C}_2\text{H}_4$ , 1h, 420 nm, bottom). The latter features the sharpest bands both in the CH stretching region ( $\nu(\text{CH}_2)$ , left) and in the  $\text{CH}_2$  bending region ( $\delta(\text{CH}_2)$ , right). The broad shoulder between  $1425$  and  $1450\text{ cm}^{-1}$  that is most pronounced in LDPE is indicative for the amorphous part in the polymer. It is almost undetectable in the spectrum of the polymer produced on the flat model catalyst indicating that it is highly crystalline.

Unfortunately possibilities for polymer characterization are very limited when working with flat model catalysts: standard techniques to determine the molecular weight distribution or the amount of methyl groups in the polymer chains ( $^{13}\text{C}$ -NMR) require at least hundred milligrams of material. We need at least a factor of 1000 higher catalytic yield than we have achieved with our current experimental setup.

We expect that the high polymerization temperature ( $160^\circ\text{C}$ ) in combination with the low polymerization pressure (1 atm) results in relatively short chains and a considerable amount of methyl branching.

On the other hand infrared spectroscopy performed in attenuated total reflection ATR mode using a spectrometer with Golden Gate accessory, shows no sign of methyl groups in the polyethylene produced on the  $\text{CrO}_x$  /  $\text{SiO}_2$  /  $\text{Si}(100)$  model catalyst (**Figure 4**) Furthermore, the extremely sharp IR-bands plus the absence of the amorphous part in the  $\delta(\text{CH}_2)$  band indicate that the polyethylene produced on the flat silica wafer is highly crystalline and that the amount of branching is small.

#### 4. How active is the $\text{CrO}_x$ / $\text{SiO}_2$ / $\text{Si}(100)$ model catalyst?

The thickness of the catalytically grown polyethylene film can readily be obtained from scalpel scratches using a Atomic force microscope (Tapping mode). Plotted against the polymerization time clearly shows a linear correlation with polymerization time, indicating a constant polymerization rate for at least the first hour of reaction<sup>[27]</sup>.

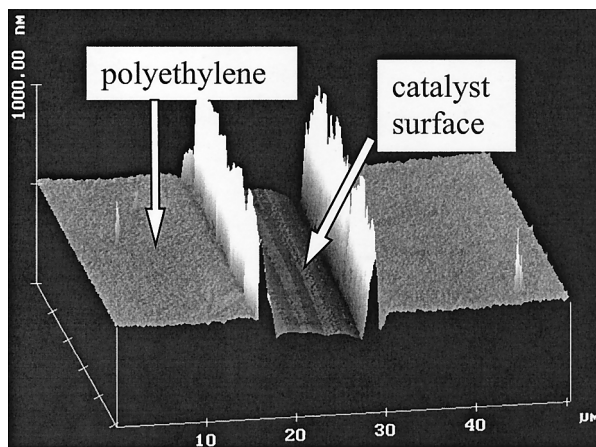


Fig. 5: AFM image of a scalpel scratch through a polyethylene film to determine the film thickness.

All the chromium on the flat silica support is molecularly dispersed and anchored to the surface and is equally accessible for the ethylene. In addition the catalytically active surface remains constant during polymerization, which is not necessarily true for porous supports that fracture during polymerization. Figure 6 shows the polymer yield versus the polymerization time for three model catalysts. They all have an initial loading of 2 Cr/nm<sup>2</sup> but have been activated at different temperatures. The polymerization activity (slope on figure 6) increases with increasing calcination temperature, just as in the industrial Phillips catalyst<sup>17)</sup>.

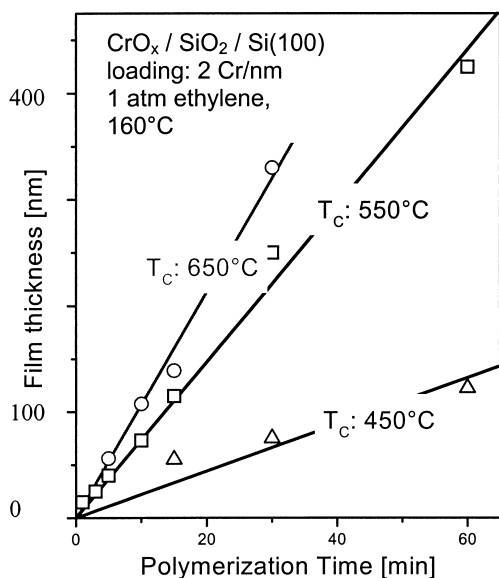


Fig. 6: The polymer yield (in nm film thickness) shows a linear correlation with polymerization time for a series of CrO<sub>x</sub> / SiO<sub>2</sub> / Si(100) model catalysts with 2 Cr/nm<sup>2</sup> and varying calcination temperature. The polymerization takes place at 160°C in 1 atm ethylene. The catalytic activity is constant during the first hour of polymerization and increases with calcination temperature.

Table 4.1. Catalytic activity of the CrO<sub>x</sub> / SiO<sub>2</sub> / Si(100) model catalyst for ethylene polymerization at 160°C and 1 bar of ethylene.

T <sub>c</sub> <sup>a</sup> [°C]	coverage <sup>b</sup> [Cr/nm <sup>2</sup> ]	Catalytic activity		
		[nm (PE) / min]	[C <sub>2</sub> H <sub>4</sub> /Cr*s] <sup>c</sup>	[g(PE)/g(cat)*h] <sup>d</sup>
450	2	2.2 ± 0.4	0.4	36
550	>1	7.4 ± 0.2	2.5	120
650	<1	10.7 ± 0.3	3.7	174

<sup>a</sup>) calcination temperature [thermal activation in O<sub>2</sub>/Ar (20/80)]

<sup>b</sup>) during calcination a portion of the catalyst loading desorbs (Figure 2)

<sup>c</sup>) pseudo turn over frequency assuming all Cr is active

<sup>d</sup>) equivalent activity of a silica support with 286 m<sup>2</sup>/g (Crossfield)

As we claim that a our  $\text{CrO}_x / \text{SiO}_2 / \text{Si}(100)$  catalyst is a realistic model of the industrial Phillips catalyst we have to prove that our catalyst achieves a realistic polymerization activity. For a calcination temperature of  $550^\circ\text{C}$  we find the polymer film growth at a rate of  $7.4 \text{ nm/min}$ . Translated to a high surface area catalyst supported on Crossfield-silica ( $286 \text{ m}^2/\text{g}$ ), the activity of our model catalyst corresponds to about 120 gram of polyethylene per gram of catalyst and per hour at 1 bar total pressure. An industrial catalyst calcined at  $500^\circ\text{C}$  produces about 1 kg of polyethylene per gram of catalyst per hour, however, in a butene slurry at  $105^\circ\text{C}$ , a total pressure of about 40 bar and an ethylene partial pressure of about 15 bar<sup>17,28,29</sup>. Szymura et al<sup>30</sup> report a polymer yield of  $25.5 \text{ g (PE) / g(catalyst)}$  for a Crossfield silica loaded with 5 wt% Cr, during polymerization at  $25^\circ\text{C}$  and atmospheric pressure in a hexane slurry, over a CO-prereduced catalyst. The precise values are difficult to compare due to differences in catalyst preparation, reaction conditions and the fracturing of the industrial catalyst, however, we conclude that the model catalyst displays a polymerization activity in the same order of magnitude as its industrial counterparts.

The anchoring of the chromate species is complete at  $450^\circ\text{C}$  and XPS/SIMS finds no clue for a further change in the chromate environment that can explain the increase in activity with increasing calcination temperature. This increase is usually attributed to a further decrease of surface-hydroxyl density upon increasing the calcination temperature. The surface hydroxyls are thought to interfere with the polymerization reaction by blocking coordination sites of the active Cr species. While this sounds plausible, to our knowledge no direct evidence for this hypothesis exists in the literature. Moreover, this standard explanation does not work for our model catalyst as the chromium loading ( $2 \text{ Cr/nm}^2$ ) was close to the saturation coverage of surface chromate for low calcination temperatures ( $1.8 - 2.3 \text{ Cr/nm}^2$ ). The surface monochromates titrates (almost) all surface hydroxyl groups, thus these cannot be blamed for the low activity of catalyst after calcination at  $450^\circ\text{C}$ . In belief that site blocking is important we propose that the chromium itself can block adsorption sites by dimerisation or clustering. This occurs when the supported surface chromates are packed too closely on the silica support. A high calcination temperature is essential for a highly active catalyst as it facilitates the redispersion of surface chromates and thus creates isolated chromium atoms which upon contact with ethylene form the active site<sup>31</sup>.

## 5. Isolated Sites

The molecularly dispersed active phase (isolated chromium atoms) is a distinctive feature of the Phillips ethylene polymerization catalyst. On our model catalyst these active sites are exposed on the flat silica surface. As we are dealing with a polymerization catalyst the reaction product (polyethylene) will remain near the active site. In a simple-minded experiment we tried to separate and visualize these active sites using catalysts with extremely low loadings (about a factor 1000 lower than the commercial catalyst). In theory (In the best of all possible worlds) the amount and size distribution of the resulting isolated polymer

island holds very desirable, atomic-level information about the reactivity of the  $\text{CrO}_x / \text{SiO}_2$  system. Figure 7 shows a catalyst with a nominal loading of  $200 \text{ Cr}/\mu\text{m}^2$  (left) as compared to a blank reference (right). Both samples were calcined at  $550^\circ\text{C}$  and then treated with 1 bar of ethylene at  $160^\circ\text{C}$  for 1h. The chromium-loaded sample contains at least 70 particles in an area of  $1 \times 1 \mu\text{m}^2$  with a threshold height higher than 1.2 nm, whereas the blank (i.e. chromium-free) reference surface remained empty. Two particles in this image are substantially larger than the others, especially in height, and these are non-spherical in shape. We assign these to polymer that has been produced by several active sites. The large majority of the polymer islands, however, appears to have spherical shape with an average height of about 2 – 3 nm. We assign these particles to polymer that has been produced by isolated active sites, which are sufficiently separated to prevent coagulation<sup>31,32</sup>.

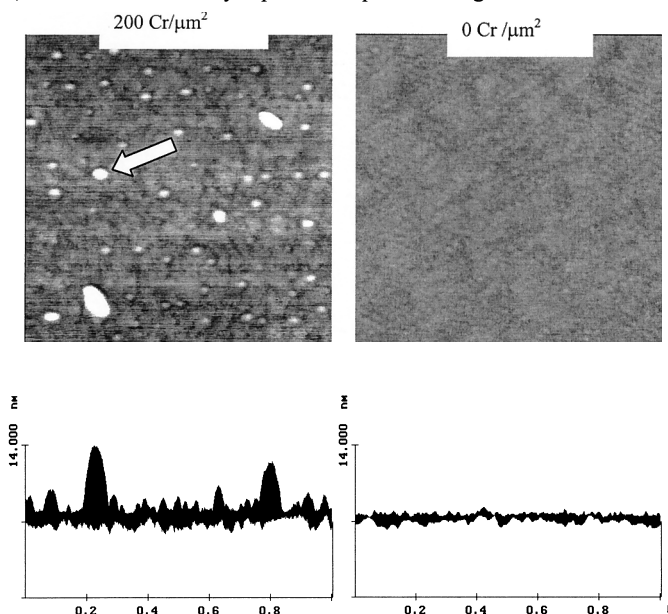


Fig. 7: AFM image ( $1 \times 1 \mu\text{m}^2$ , height contrast, topview and sideview) of two model-catalysts after polymerization ( $160^\circ\text{C}$ , 1h). Left: loading  $200 \text{ Cr}/\mu\text{m}^2$  resulting in at least 70 PE islands of at least 1.2 nm in height. Right: blank reference with average roughness of 0.5 nm without any island higher than 1 nm. The arrow marks the polymer island discussed in Figure 8.

We can use AFM to estimate the catalytic activity of the individual active sites on the  $\text{CrO}_x / \text{SiO}_2 / \text{Si}(100)$  model catalyst as illustrated in figure 8. The AFM tip with a tip-radius of 5 nm overestimates the particle diameter by only 1-2 nm. Assuming the polymer island in figure 8 has been produced by an isolated active site of one chromium atom, we calculate the turnover

frequency of this site to be  $17 \pm 2$   $\text{C}_2\text{H}_4/(\text{Cr}^*\text{s})$ . The polymer island in this example is relatively big, the average turnover frequency determined from 25 polymer islands on figure 7 results in  $6.6$   $\text{C}_2\text{H}_4/(\text{Cr}^*\text{s})$ , again assuming that they are the product of isolated chromium sites.

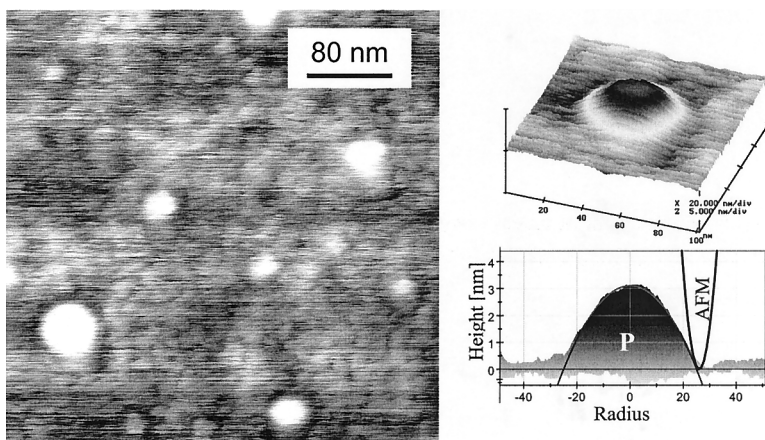


Fig. 8: 400x400 nm zoom of figure 7. The polymer island marked in figure 7 has a paraboloid shape, with a diameter of  $48 \pm 2$  nm and a height of  $3.1 \pm 0.2$  nm. This corresponds to a volume of about  $2800 \text{ nm}^3$ . Assuming that the polymer has been produced by a single active site, we calculate its activity (average turn- over frequency over the 1 hour polymerization run) to be  $17 \pm 2$  molecules ( $\text{C}_2\text{H}_4$ ) per chromium atom and per second. The AFM tip shown for comparison is of paraboloid shape and has a tip radius of 5 nm.

At this stage it is difficult to judge how far deactivation of some of the active sites or coalescence of some of the isolated polymer islands corrupt the information about the catalytic activity that can be deduced from these pictures. Nevertheless we conclude that it is possible to produce and visualize isolated polymerization sites on the  $\text{CrO}_x / \text{SiO}_2 / \text{Si}(100)$  model catalyst using AFM and that we can even quantify their catalytic yield.

## 6. Conclusions and Outlook

In this article we investigated the influence of the calcination temperature on the polymerization activity of the  $\text{CrO}_x/\text{SiO}_2$ -system (Phillips catalyst) using a flat model catalyst, following the industrial preparation as closely as possible. Our model system reproduces the expected behavior known from its high surface-area counterparts: the catalytic activity of the model catalyst increases with increasing calcination temperature.

We attribute this increase in activity to the isolation of monomeric chromium species in the silica support, preventing deactivation of the coordinatively unsaturated active species through dimerisation (clustering).

Individual active sites can be visualized with AFM if the chromium loading is drastically reduced. They produce small polyolefin islands, which can be used to determine the catalytic activity of the underlying chromium atom.

Though there is quite some work ahead to obtain statistically meaningful results this approach offers a unique chance to study the reactivity of a heterogenous catalytic system on a per site basis.

## Acknowledgement

This work has been performed under the auspices of NIOK, the Netherlands Institute for Catalysis Research and the Dutch Polymer Institute (DPI) with financial support from the Netherlands Technology Foundation (STW).

## References

1. P.L.J. Gunter, J.W. Niemantsverdriet, F.H. Ribeiro, G.A. Somorjai, *Catal.Rev-Sci.and Eng.* **39**, 77 (1997)
2. W. Goodman, *Chem.Rev.* **95**, 523 (1995)
3. J.W. Niemantsverdriet, *Spectroscopy in Catalysis, an Introduction* (Wiley-VCH, Weinheim, 2000)
4. G.A. Somorjai, *Cattech* **3** (1),84 (1999)
5. F. Rumpf, H. Poppa, M. Boudart, *Langmuir.* **4**, 722 (1988)
6. F.H. Ribeiro, G.A. Somorjai, *Receuil des Travaux Chimiques des Pays-Bas* **113**, 419 (1994)
7. M.X. Xang, P.W. Gracias, P.W. Jacobs, G.A. Somorjai, *Langmuir.* **14**, 1458 (1998)
8. I. Zuburticudis, H. Saltsburg, *Science* **258**, 1337 (1992)
9. E. Magni and G.A. Somorjai, *Surface Science*, **345**, 1 (1996)
10. E.W. Kuipers, C. Laszlo, W. Wieldraaijer, *Catal.Lett.* **17**, 71 (1993)
11. E.W. Kuipers, C. Doornkamp, W. Wieldraaijer, R.E. van den Berg, *Chem.Mat.* **5**, 1367 (1993)
12. R.M. van Hardeveld, P.L.J. Gunter L.J. van IJzendoorn, W. Wieldraaijer, E.W. Kuipers, J.W. Niemantsverdriet *Appl.Surf.Sci.* **84**, 339 (1995)
13. J.W. Niemantsverdriet, A.F.P. Engelen, A.M. de Jong, W. Wieldraaijer, G.J. Kramer, *Appl.Surf.Sci.* **144-145**, 366 (1999)
14. H.L. Krauss and H. Stach, *Z.Anorg.Alg.Chem.* **366**, 280 (1969)
15. A.M. de Jong, V.H.J. de Beer, J.A.R. van Veen, J.W. Niemantsverdriet, *J.Phys.Chem.* **100**: 17722 (1996)
16. J.P. Hogan, R.J. Banks, US-Patent 2,825,721. (1958)
17. M.P. McDaniel, *Adv.Catal.* **33**, 47(1985)
18. B.M. Weckhuysen, I.E. Wachs, R.A. Schoonheydt, *Chem.Rev.* **96**: (8),3327 (1996)

19. J.P. Hogan, *J.Polym.Sci.,Part A-1* **8**, 2637 (1970)
20. A. Zechina, E. Garrone, G. Ghiotti, C. Morterra, E. Borello, *J.Phys.Chem.* **79** (10), 966 (1965)
21. M.P. McDaniel, *J.Catal.* **67**, 71 (1981)
22. B.M. Weckhuysen, *et al*, *J.Chem.Soc.Faraday Trans.* (1995) Vol **91**(1). **83**, 245 (1995)
23. B.M. Weckhuysen, L.M. De Ridder, R.A. Schoonheydt, *J.Phys.Chem.* **97**, 4756 (1993)
24. P.C. Thüne, C.P.J. Verhagen, M.J. Van den Boer, J.W. Niemantsverdriet, *J.Phys.Chem.B* **101**, 8559 (1997)
25. P.C. Thüne, J.W. Niemantsverdriet, *Isr. J.Chem.* **38**, 385 (1998)
26. P.C. Thüne, R. Linke, W.J.H. van Gennip, A.M. de Jong and J.W. Niemantsverdriet, *J.Phys.Chem.B* **105**, 3073 (2001)
27. P.C. Thüne, J. Loos, P.J. Lemstra, J.W. Niemantsverdriet, *J.Catal.* **183** ( 1),1 (1999)
28. K.-T. Choi, W.H. Ray, *J.Macromol.Sci.Macromol.Chem.Phys.* **C25**: 1 (1985)
29. R. Merryfield, M.P. McDaniel, G. Parks, *J.Catal.* **77**, 348 (1982)
30. J.A. Szymura, I.G. Dalla Lana, R. Fiedorow, P.A. Zielinski, *Macromolecules* **29**, (9),3103 (1996)
31. P.C. Thüne, J.Loos, P.J. Lemstra and J.W. Niemantsverdriet, *Top.Catal.* **13**, 67 (2000)
32. P.C. Thüne, J.Loos, P.J. Lemstra and J.W. Niemantsverdriet, *submitted to J. Am. Chem. Soc.*